Deformation-based shape control with a multirobot system

Miguel Aranda, Juan Antonio Corrales and Youcef Mezouar

Abstract— **We present a novel method to control the relative positions of the members of a robotic team. The application scenario we consider is the cooperative manipulation of a deformable object in 2D space. A typical goal in this kind of scenario is to minimize the deformation of the object with respect to a desired state. Our contribution, then, is to use a global measure of deformation directly in the feedback loop. In particular, the robot motions are based on the descent along the gradient of a metric that expresses the difference between the team's current configuration and its desired shape. Crucially, the resulting multirobot controller has a simple expression and is inexpensive to compute, and the approach lends itself to analysis of both the transient and asymptotic dynamics of the system. This analysis reveals a number of properties that are interesting for a manipulation task: fundamental geometric parameters of the team (size, orientation, centroid, and distances between robots) can be suitably steered or bounded. We describe different policies within the proposed deformation-based control framework that produce useful team behaviors. We illustrate the methodology with computer simulations.**

I. INTRODUCTION

Compared to a single robot, a multirobot team can manipulate larger and heavier objects and provide more refined and precise behaviors. The team's actions when manipulating a rigid or deformable body must be carefully coordinated, to avoid damaging it and encountering unpredictable motions [1]–[3]. In particular, the robots typically need to ensure that the object remains close to a desired state. In this paper, we consider a scenario where a team of robots grasps rigidly a deformable object in 2D. We assume that the desired state of the object is encapsulated by a desired shape of the team. This assumption is reasonable in different practical cases, e.g.: 1) The polygon joining the grasping points represents the object's contour faithfully enough. 2) The object is highly deformable and thus its shape adapts to the team's shape. 3) The task does not require precise object shape control but, e.g., making the object fit in a given region of space. 4) The required object deformation is small.

Therefore, we propose a method to control the shape of the robotic team. The approach minimizes a measure of the team's deformation relative to its desired shape. In this way, the controller aligns with the usual goal of keeping the manipulated object close to a desired state. Our measure of deformation is the function that one minimizes when solving

a certain Procrustes shape alignment problem [4]. In 2D space, the particular problem where rotation and scaling are optimized admits a closed-form solution. Our insight and contribution here is to appropriately formalize this solution and to define a gradient control strategy based on it. The controller is simple to compute, and amenable to analysis. Notably, we identify interesting properties for a manipulation task: the dynamics of the team's size, centroid and orientation can be controlled suitably both in short-term and asymptotic time scales. The robots' motions are tightly coordinated – as is typically desired in manipulation tasks–, balanced and efficient, and the distances between them can be bounded (to avoid overstretching, over-squeezing or collisions). We analyze these points and illustrate them via simulations.

A. Related work

Precise knowledge of object deformation is not a fundamental consideration for some multirobot manipulation approaches which deal with objects that are either essentially rigid [1], [3], [5]–[9] or, on the other hand, highly deformable. In the latter case, it may be sufficient to simply respect upper and lower inter-robot distance bounds [10], [11]. To ensure that the relative states of the robots maintain desired values, these approaches often exploit distributed techniques such as consensus or formation control [12], which are very successful in many scenarios. Typically, they possess strong asymptotic convergence properties, but short-term team dynamics are difficult to predict. Contrary to this literature, our method is based on a concept of global shape of the team. This creates closely coordinated motions, which is a singularly relevant property when the robots are manipulating a deformable object.

The robotic manipulation of deformable objects is a highly active area of research where a variety of methodologies, tasks, robotic platforms and object types have been considered [13]. To keep the object's geometry under control, existing works typically exploit a certain degree of knowledge about how it deforms under the action of the robots. Some authors have used a prior model of the object's deformation [14], [15]. The models depend greatly on the type of object; linear objects, for instance, admit representations suitable for shape planning [16], [17]. Other authors favor model-free approaches [2], [18], in some cases using a *deformation Jacobian* estimated online from sensory data [19]–[21]. For feedback control, methods not reliant on prior models are considered more generalizable and computationally simpler. The methods cited in the paragraph have these general traits: 1) When multiple robots are used, the robots share a common global goal (e.g., object shape control), but they

do not coordinate their motions with one another. In contrast, our method emphasizes the coordination/synchronization of the robots' actions. This can lead to higher efficiency in the team's motions; 2) The target configuration the robots pursue (e.g., corresponding to a desired object shape) is *anchored*, to the workspace or to a reference frame. In contrast, in our approach the target configuration is the one that minimizes, for the *current* configuration of the robots, the team's deformation measure. The motions are therefore not linked to external references and, being based purely upon deformation, they produce more efficient changes of shape. In addition, a free-floating target configuration –which our method provides– is adaptable and flexible for object transportation tasks. Furthermore, maintaining a minimum deformation can minimize damages to the object, and to the robots, because the contact forces will be reduced.

Finally, Procrustes-based deformation metrics similar to the one we exploit –which appear frequently in shape alignment problems [22]– have been used previously to control mobile robot formations [23], estimate their error [24], or determine optimal a priori destination formations [25]. To our knowledge, this is the first work to study the application of such metrics to cooperative manipulation tasks.

II. GENERAL PROBLEM STATEMENT

Consider a set, $\mathcal{N} = \{1, 2, ..., N\}$, $N > 1$, of robots with the ability to move as kinematic point masses satisfying:

$$\dot{\mathbf{q}}_\mathbf{i} = \mathbf{u}_\mathbf{i}, \ \ \forall i \in \mathcal{N} \tag{1}$$

(boldface font is used for multidimensional variables), where $\mathbf{q}_\mathbf{i} \in \mathbb{R}^2$ denotes robot $i's$ position in a given reference frame and $\mathbf{u}_\mathbf{i} \in \mathbb{R}^2$ its control input. We will in general not notate time dependence. $\{\cdot\}$ will stand for $\{\cdot \mid i \in \mathcal{N}\}$. The norm used in this paper is the Euclidean one. Our focus is on a scenario where the robots manipulate an object on a plane, each of them grasping it rigidly at a fixed contact point on the object's contour. Similar setups with free-floating rigid-grasping robotic actuators are assumed in, e.g., [2], [14], [20]. We use the following notation for the relative position vectors: $\mathbf{q}_{\mathbf{ij}} = \mathbf{q}_\mathbf{i} - \mathbf{q}_\mathbf{j}$. We also work with a prescription of a desired geometry for the robotic team. This desired geometry is considered to be constant over time. It can be encapsulated by a layout of points $\mathbf{c}_\mathbf{i} \in \mathbb{R}^2$ in the workspace: $\{\mathbf{c}_\mathbf{i}\}$. We assume that $\mathbf{c}_\mathbf{i} \neq \mathbf{c}_\mathbf{j}$ for at least two distinct robots $i, j \in \mathcal{N}$. We define the centroid of the current robot positions as $\mathbf{q_o}$, and the centroid of the desired geometry as $\mathbf{c_o}$.

We assume that the state of the object is defined by the configuration of the robotic team. Hence, we focus on controlling the team. We do *not* control the state of the object's full contour. This assumption is justified in the first paragraph of the paper. Still, one cannot ignore that there is an object being handled by the robots: this demands the team's motions to be closely coordinated and stable, and to satisfy size and distance bounds. Our deformation-based control approach allows to conform with these requirements.

We address the problem of *shape control*, defined as making $\{\mathbf{q}_\mathbf{i}\}$ satisfy $\mathbf{q}_\mathbf{i} = s\mathbf{R}\mathbf{c}_\mathbf{i} + \mathbf{t} \ \forall i \in \mathcal{N}$ for some scaling

$s \in \mathbb{R}_{\geq 0}$, rotation $\mathbf{R} \in SO(2)$, and translation $\mathbf{t} \in \mathbb{R}^2$. This condition implies that the team has the same shape as the desired geometry. Next, we describe the proposed solution.

III. CONTROL STRATEGY

Let us consider the following function defined from the two given point sets $\{\mathbf{q}_\mathbf{i}\}$ and $\{\mathbf{c}_\mathbf{i}\}$:

$$\gamma_g = \frac{1}{2} \sum_{i \in \mathcal{N}} ||\mathbf{q}_\mathbf{i} - \mathbf{H_g}\mathbf{c}_\mathbf{i} + \mathbf{t_g}||^2, \tag{2}$$

where $\mathbf{H_g} \in \mathbb{R}^{2 \times 2}$ is a Euclidean similarity transformation –comprising rotation and uniform scaling–, and $\mathbf{t_g} \in \mathbb{R}^2$ is a translation offset. γ_g is a measure of the SSD (Sum of Squared Differences) error between the points in the sets when the points in $\{\mathbf{c}_\mathbf{i}\}$ are rotated and scaled by $\mathbf{H_g}$, and translated by $\mathbf{t_g}$. Finding the optimal $\mathbf{H_g}$ and $\mathbf{t_g}$ (i.e., the similarity and offset that minimize γ_g for two given sets) is a type of Procrustes shape-fitting problem [4]. One can see that the optimal offset corresponds with making the centroid of the two point sets coincide. Therefore, we henceforth use $\mathbf{q_{io}}$ and $\mathbf{c_{io}}$ in (2), and choose $\mathbf{t_g} = \mathbf{0}$.

Let us define a similarity $\mathbf{H} \in \mathbb{R}^{2 \times 2}$ having the form:

$$\mathbf{H} = \begin{bmatrix} h_1 & -h_2 \\ h_2 & h_1 \end{bmatrix} \tag{3}$$

$$h_1 = \frac{1}{c_s} \sum_{i \in \mathcal{N}} \mathbf{q_{io}^T}\mathbf{c_{io}}$$

$$h_2 = \frac{1}{c_s} \sum_{i \in \mathcal{N}} \mathbf{q_{io}^T}\mathbf{c_{io}^\perp},$$

where $c_s = \sum_{i \in \mathcal{N}} ||\mathbf{c_{io}}||^2$, i.e., a strictly positive constant scalar, and the operator $\perp$ on a 2D vector $\mathbf{a}$ is defined as a counterclockwise rotation of $\pi/2$ radians: $\mathbf{a}^\perp = [(0,1)^T, (-1,0)^T]\mathbf{a}$. It can be verified with simple manipulations that $\frac{\partial \gamma_g}{\partial \mathbf{H_g}(1,1)}\rfloor_{\mathbf{H_g}(1,1)=h_1} = 0$ and $\frac{\partial \gamma_g}{\partial \mathbf{H_g}(2,1)}\rfloor_{\mathbf{H_g}(2,1)=h_2} = 0$ and, via the second derivative test, that h_1 and h_2 are unique *minimizers* of γ_g. Thus, the optimal choice in (2) is $\mathbf{H_g} = \mathbf{H}$.

Taking the above into consideration, our control approach rests on the following cost function:

$$\gamma = \frac{1}{2} \sum_{i \in \mathcal{N}} ||\mathbf{q_{io}} - \mathbf{H}\mathbf{c_{io}}||^2. \tag{4}$$

Let us highlight that h_1 and h_2 satisfy $\frac{\partial \gamma}{\partial h_1} = 0$ and $\frac{\partial \gamma}{\partial h_2} = 0$. A visual interpretation of the cost function in the context of the shape control problem addressed is given in Fig. 1. We discuss important aspects about the chosen function next.
1) A crucial fact to notice is that γ can be interpreted directly as a measure of the deformation relative to the desired shape of the robotic team. $\mathbf{H}$ is such that $\{\mathbf{H}\mathbf{c_{io}} + \mathbf{q_o}\}$ is the closest (in terms of the SSD in γ_g) possible team configuration to $\{\mathbf{q}_\mathbf{i}\}$ having the same shape as $\{\mathbf{c}_\mathbf{i}\}$. The SSD for this optimal configuration is γ, which therefore quantifies purely how much the shape of $\{\mathbf{c}_\mathbf{i}\}$ is deformed in the current configuration $\{\mathbf{q}_\mathbf{i}\}$. Then, our controller, based on the gradient of γ, *directly minimizes the deformation* with
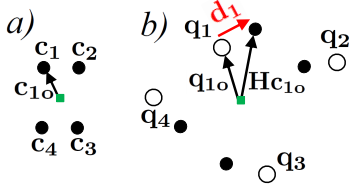
Fig. 1. Illustration of control strategy with four robots. Only the vectors for one robot ($i = 1$) are shown. The vectors for the other robots are analogous. The centroids are marked as squares. *a)* Desired geometry $\{\mathbf{c_i}\}$. *b)* Current robot positions $\{\mathbf{q_i}\}$ (hollow circles) and desired geometry in *a)* transformed by the optimal similarity $\mathbf{H}$ (3). $\mathbf{H}$ rotates and uniformly scales every $\mathbf{c_{io}}$. Therefore, the point set $\{\mathbf{Hc_{io}}\}$ has the same shape as $\{\mathbf{c_{io}}\}$. Notice that $\gamma = (1/2)\sum_{i \in \mathcal{N}} ||\mathbf{d_i}||^2$. $\mathbf{d_i}$ is robot i's motion vector, opposite to the gradient of γ with respect to $\mathbf{q_i}$, as explained in the text.

respect to the desired shape. This is particularly appropriate for a task of manipulation of a deformable object.

2) γ is very suitable for our purpose: it is differentiable and simple computationally –which is important for feedback control–. It expresses unequivocally the achievement of the prescribed shape, and its gradients have closed-form expressions. Fundamental parameters (size, rotation and centroid of the team) can be steered and controlled, and exhibit dynamic behaviors that are interesting for manipulation tasks.

3) Since we use a similarity ($\mathbf{H}$), the desired physical *size* of the team is unprescribed, which may appear suboptimal or even risky. Various arguments support our choice: having the size parameter as a degree of freedom provides adaptability to changing task requirements or environment conditions, allowing to take advantage of the deformability of soft objects. Also, the similarity (3) is linear in the relative position coordinates, and this makes it easier to uncover its interesting dynamic properties. Finally, as we will show, the value of the team's size can still be controlled.

Let us define the scaling, s_h, and rotation, $\mathbf{R_h}$, encapsulated by $\mathbf{H}$. The control strategy does not use these parameters, but they provide us with a physical interpretation of the action of the matrix. We can write $\mathbf{H} = s_h \mathbf{R_h}$, with:

$$s_h = \sqrt{h_1{}^2 + h_2{}^2}, \tag{5}$$

$$\mathbf{R_h} = \begin{bmatrix} \cos(\alpha_h) & -\sin(\alpha_h) \\ \sin(\alpha_h) & \cos(\alpha_h) \end{bmatrix}, \quad \alpha_h = atan2(h_2, h_1), \tag{6}$$

being by our definition $\alpha_h = 0$ when $h_1 = h_2 = 0$. Notice that there is no discontinuity in this alternative representation of $\mathbf{H}$, because when $h_1 = h_2 = 0$, it holds that $s_h = 0$.

The size of the team is an essential property to take into account. We define it as the quadratic mean of the robots' distances to the centroid. The size of the configuration towards which the robots move at a given instant (which can be termed *destination configuration*) is thus defined as:

$$s_d = \sqrt{\frac{1}{N} \sum_{i \in \mathcal{N}} ||\mathbf{Hc_{io}}||^2} = s_h \sqrt{\frac{c_s}{N}}. \tag{7}$$

Observe that, as c_s and N are constant, s_d and s_h are essentially equivalent ways of expressing this size. Similarly,

we define the size of the *current configuration* as:

$$s_q = \sqrt{\frac{1}{N} \sum_{i \in \mathcal{N}} ||\mathbf{q_{io}}||^2}. \tag{8}$$

We can already formulate a result that supports γ as being an appropriate cost function for our control purposes.

Lemma 1: $\{\mathbf{q_i}\}$ is equal to $\{\mathbf{c_i}\}$ up to translation, rotation and scaling if and only if $\gamma = 0$.

One can prove this lemma by considering the form of (3).

We compute next the gradient of γ with respect to the position of one of the robots $i \in \mathcal{N}$. Recall that the matrix $\mathbf{H}$ satisfies $\frac{\partial \gamma}{\partial h_1} = 0$ and $\frac{\partial \gamma}{\partial h_2} = 0$. Therefore, the gradient will be given directly by the partial derivative with respect to $\mathbf{q_i}$. In particular, it has the following expression:

$$\nabla_{\mathbf{q_i}} \gamma = \frac{\partial \gamma}{\partial \mathbf{q_i}} = \sum_{j \in \mathcal{N}} (\mathbf{q_{jo}} - \mathbf{Hc_{jo}})^T \frac{\partial \mathbf{q_{jo}}}{\partial \mathbf{q_i}} =$$

$$(1 - \frac{1}{N})(\mathbf{q_{io}} - \mathbf{Hc_{io}}) - \frac{1}{N} \sum_{\substack{j \in \mathcal{N} \\ j \neq i}} \mathbf{q_{jo}} - \mathbf{Hc_{jo}} = \mathbf{q_{io}} - \mathbf{Hc_{io}},$$

$$\tag{9}$$

where we have separated in two different terms the case $j = i$ and the case $j \neq i$, and used the fact that the centroids satisfy: $\mathbf{q_o} = \sum_{i \in \mathcal{N}} \mathbf{q_i}/N$, $\mathbf{c_o} = \sum_{i \in \mathcal{N}} \mathbf{c_i}/N$.

A. Standard control law

For each robot, we define its standard control law in the direction opposite to the gradient of γ. The *motion vector* for robot i takes, from (9), the form that follows:

$$\mathbf{d_i} = -\nabla_{\mathbf{q_i}} \gamma = \mathbf{q_{oi}} - \mathbf{Hc_{oi}}. \tag{10}$$

This vector can be directly visually interpreted in Fig. 1. We propose the following control law for each robot $i \in \mathcal{N}$:

$$\mathbf{u_i} = k_i \mathbf{d_i}, \tag{11}$$

where $k_i \geq k_{min}$ (k_{min} being a positive constant) is a gain, constant or smoothly time-varying. The information needed to implement this control law is $\mathbf{q_{oi}} \; \forall i \in \mathcal{N}$, which can be obtained from measurements of the relative positions of the team's robots. It can be seen (we omit the details for brevity) that this controller can be computed in a local reference frame. Note that $\mathbf{H}$ in (10) is a *feedback* matrix, recomputed *at every instant* according to (3). The controller has a closed-form expression and, being based on minimizing a globally defined metric, it needs knowledge about *all the robots*.

IV. CONTROLLER ANALYSIS

Let us inspect how the multirobot system behaves under the controller. We first state a necessary assumption.

Assumption 1: s_q remains upper-bounded for all time. We now study the stability with respect to the desired shape.

Theorem 1: Under the action of the control law (11), the robots converge exponentially to a configuration in which they form the desired shape and stay static.

Proof: As s_q is upper-bounded under the controller (see Assumption 1), the relative positions of the robots remain

finite (8). We choose γ as candidate Lyapunov function, and analyze its dynamics when the controller (11) is in operation:

$$\dot{\gamma} = \sum_{i \in \mathcal{N}} (\nabla_{\mathbf{q_i}} \gamma)^T \dot{\mathbf{q_i}} = -\sum_{i \in \mathcal{N}} k_i(t) ||\mathbf{d_i}||^2$$
$$\leq -k_{\min} \sum_{i \in \mathcal{N}} ||\mathbf{d_i}||^2 = -2k_{\min}\gamma. \qquad (12)$$

From LaSalle's invariance principle, one can see that the system converges exponentially to a configuration in which $\gamma = 0$, i.e., where the robots are in the desired shape (Lemma 1). In addition, $\gamma = 0$ implies $\mathbf{d_i} = \mathbf{0}$ and thus, $\mathbf{u_i} = \mathbf{0}$ $\forall i \in \mathcal{N}$, i.e., the robots' velocities converge to zero. ∎

Remark 1: The exponential decay of γ (12) implies that the robot speeds vanish exponentially. Since these speeds are thus integrable as time goes to infinity, the inter-robot distances will remain finite. We support Assumption 1 with this observation and with the analysis of the dynamics of s_q provided in the following sections.

A. Properties of team size, rotation and centroid

It is essential to have some insight on how the team size is expected to evolve. Let us state a relevant result:

Lemma 2: The cost function γ (4) can be expressed as:

$$\gamma = \frac{N}{2}(s_q{}^2 - s_d{}^2). \qquad (13)$$

Proof: The proof relies on algebraic manipulations of (4). We omit the details, for brevity. ∎

There is an interesting fact to notice here: γ expresses – as highlighted previously– the *difference in shape*; but, as (13) shows, it additionally encapsulates the *difference in size* between the current and destination configurations. By minimizing γ, one is controlling size and shape simultaneously. We can state the following property regarding team sizes:

Proposition 1: It holds that $s_d \leq s_q$ for any current and desired configurations of the robots.

Proof: As $\gamma \geq 0$, (13) proves the result. ∎

This means that the controller naturally moves the robots towards a configuration in which the size of the team is never larger than its current size. This suggests an interesting trend towards maintaining the *energy* of the system and avoiding divergent behaviors of the team. On a more practically specific note, this property can also be useful so as to prevent object overstretching. A result on the dynamics of $\mathbf{H}$ follows.

Proposition 2: If all robots apply the control law (11) with the same gain k_c, then $\mathbf{H}$ remains constant over time.

Proof: We examine the time-derivative of $\mathbf{H}$:

$$\dot{h}_1 = \sum_{i \in \mathcal{N}} \frac{\partial h_1}{\partial \mathbf{q_i}}^T \dot{\mathbf{q_i}}. \qquad (14)$$

We can find that $\frac{\partial h_1}{\partial \mathbf{q_i}} = \mathbf{c_{io}}/c_s$, and substitute (11) to get:

$$\dot{h}_1 = \frac{k_c}{c_s} \sum_{i \in \mathcal{N}} \mathbf{c_{io}^T}(\mathbf{q_{oi}} - \mathbf{Hc_{oi}})$$
$$= -\frac{k_c}{c_s}(\sum_{i \in \mathcal{N}} \mathbf{q_{io}^T c_{io}} - \sum_{i \in \mathcal{N}} \mathbf{c_{io}^T Hc_{io}}). \qquad (15)$$

Using that $\mathbf{H}$ is a similarity and substituting its expression (3), the last term of (15) can be readily seen to be:

$$\sum_{i \in \mathcal{N}} \mathbf{c_{io}^T Hc_{io}} = \sum_{i \in \mathcal{N}} (\frac{||\mathbf{c_{io}}||^2}{c_s} \sum_{j \in \mathcal{N}} \mathbf{q_{jo}^T c_{jo}}) = \sum_{i \in \mathcal{N}} \mathbf{q_{io}^T c_{io}}. \qquad (16)$$

Hence, $\dot{h}_1 = 0$. An analogous analysis can be used to show that $\dot{h}_2 = 0$ and, therefore, $\mathbf{H}$ remains constant. ∎

Thus, both s_h and $\mathbf{R_h}$ remain constant. This fact can actually facilitate the motion of the robots during the task, and help them attain efficiently the desired shape while avoiding unnecessary rotations/re-scalings of the object.

When all robots employ the same gain, the team's centroid is preserved under the action of the controller. One can verify this readily from (11) and realizing that by definition the sums of all N vectors $\mathbf{q_{oi}}$ or $\mathbf{c_{oi}}$ are zero. Thus:

$$\dot{\mathbf{q_o}} = \frac{1}{N} \sum_{i \in \mathcal{N}} \dot{\mathbf{q_i}} = \frac{k_c}{N}(\sum_{i \in \mathcal{N}} \mathbf{q_{oi}} - \mathbf{H} \sum_{i \in \mathcal{N}} \mathbf{c_{oi}}) = \mathbf{0}. \qquad (17)$$

This fact is useful for navigation/transportation problems where we want to steer the centroid of the team: this centroid motion objective can be decoupled from the motions of the shape controller. Another important conclusion is that the changes in the manipulated object's shape are *balanced*, because they do not displace the center of the contact points.

B. Inter-robot distance bounds

Upper and lower inter-robot distance bounds are of great importance in practice because they can ensure that overstretching and over-squeezing/collisions, respectively, are avoided. To study this issue, let us first state a useful result.

Lemma 3: The following function:

$$\gamma_p = \frac{1}{2} \sum_{i \in \mathcal{N}} \sum_{j \in \mathcal{N}} ||\mathbf{q_{ij}} - \mathbf{Hc_{ij}}||^2 \qquad (18)$$

satisfies $\gamma_p = 2N\gamma$.

Proof: Defining $\mathbf{v_i} = \mathbf{q_{io}} - \mathbf{Hc_{io}}$, we have that $\gamma = \frac{1}{2} \sum_{i \in \mathcal{N}} ||\mathbf{v_i}||^2$ and $\gamma_p = \frac{1}{2} \sum_{i \in \mathcal{N}} \sum_{j \in \mathcal{N}} ||\mathbf{v_{ij}}||^2 = 2N\gamma - v_{ij}$, where $v_{ij} = \sum_{i \in \mathcal{N}} \sum_{j \in \mathcal{N}} \mathbf{v_i^T v_j} = \sum_{i \in \mathcal{N}} \mathbf{v_i^T} \sum_{j \in \mathcal{N}} \mathbf{v_j}$. Notice that by definition $\sum_{i \in \mathcal{N}} \mathbf{v_i} = \mathbf{0}$. Thus, $v_{ij} = 0$ and the stated result follows. ∎

Unlike γ, the function γ_p is defined in terms of the pairwise inter-robot vectors. As both functions are equal up to a constant multiplicative factor, we can use γ to define bounds for the pairwise distances. Let us define the variable $e(t) = 2\sqrt{N}\sqrt{\gamma(t)}$. We can state the property that follows.

Proposition 3: The distance at time t between any two robots $i \in \mathcal{N}$, $j \in \mathcal{N}$ is bounded as follows:

$$s_h(t)||\mathbf{c_{ij}}|| - e(t) \leq ||\mathbf{q_{ij}}(t)|| \leq s_h(t)||\mathbf{c_{ij}}|| + e(t). \qquad (19)$$

Proof: One can substitute (4), (18), and use the triangle inequality to obtain the result. ∎

Thus, by ensuring that γ and s_h maintain suitable values, one has a means to keep the inter-robot distances bounded.

V. Variants of the controller

Modifications of the controller (11) are presented next. These variants retain the underlying idea of maintaining the deformation under control, by minimizing γ. At the same time, they provide different dynamic behaviors, or allow to fix important geometric parameters, accommodating constraints that are relevant in practical applications.

A. Team motions in the rotation and scaling nullspaces

We next describe alternative control laws that preserve either the rotation or the scaling encapsulated in $\mathbf{H}$. They are found by exploiting the nullspaces of these parameters.

1) Rotation-preserving motions: We define them as those for which $\dot{\mathbf{R}}_{\mathbf{h}} = 0$. We can provide the following result.

Proposition 4: A motion strategy where the robots implement the control law that follows:

$$\mathbf{u_i} = k_c(\mathbf{q_{oi}} - w_i(t)\mathbf{Hc_{oi}}),\ w_i(t) \in \mathbb{R}_{>0},\ \forall i \in \mathcal{N}, \quad (20)$$

is rotation-preserving.

Proof: Let us express (20) for each robot as $\mathbf{u_i} = \mathbf{u_i^s} + \mathbf{u_i^n}$, where $\mathbf{u_i^s}$ is the standard control law (11). Then:

$$\mathbf{u_i^n} = k_c w_i^*(t)\mathbf{Hc_{oi}},\ \forall i \in \mathcal{N}, \quad (21)$$

with $w_i^*(t) = 1 - w_i(t)$ a scalar. We will compute next the dynamics of h_1 and h_2. From Proposition 2 we know that both terms are constant under $\mathbf{u_i^s}$. Thus, we have, for h_1:

$$\dot{h}_1 = \sum_{i \in \mathcal{N}} \frac{\partial h_1}{\partial \mathbf{q_i}}^T \mathbf{u_i^n} = \frac{k_c}{c_s} \sum_{i \in \mathcal{N}} \mathbf{c_{io}^T} w_i^*(t)\mathbf{Hc_{oi}} = \frac{k_c}{c_s}w(t)h_1,$$

$$(22)$$

with $w(t) = -\sum_{i \in \mathcal{N}} w_i^*(t)\|\mathbf{c_{io}}\|^2$. Analogously, for h_2:

$$\dot{h}_2 = \sum_{i \in \mathcal{N}} \frac{\partial h_2}{\partial \mathbf{q_i}}^T \mathbf{u_i^n} = \frac{k_c}{c_s} \sum_{i \in \mathcal{N}} \mathbf{c_{io}^{\perp T}} w_i^*(t)\mathbf{Hc_{oi}} = \frac{k_c}{c_s}w(t)h_2.$$

$$(23)$$

We assume the angle α_h (6) is always well-defined, which it will be as long as the scaling satisfies $s_h > 0$. We can express its dynamics as $\dot{\alpha}_h = (h_1\dot{h}_2 - \dot{h}_1 h_2)/s_h^2$. Hence, substituting (22) and (23), it is concluded that $\dot{\alpha}_h = 0$. ∎

This is interesting because if the object does not rotate, the manipulating robots' motions are more efficient and balanced. Also, a robot could use the degree of freedom given by $w_i(t)$ to satisfy other task criteria (i.e., avoid obstacles, or steer the normal of the object's contour).

2) Scale-preserving motions: These are team motions for which $\dot{s}_h = 0$. We find the result that follows.

Proposition 5: The following team motion policy:

$$\mathbf{u_i} = k_c((\mathbf{q_{oi}} - \mathbf{Hc_{oi}}) + z_i(t)\mathbf{Hc_{oi}^{\perp}}),\ z_i(t) \in \mathbb{R},\ \forall i \in \mathcal{N}, \quad (24)$$

is scale-preserving.

Proof: Let us write (24) for each robot as $\mathbf{u_i} = \mathbf{u_i^s} + \mathbf{u_i^m}$, where $\mathbf{u_i^s}$ is the standard control law (11). Then:

$$\mathbf{u_i^m} = k_c z_i(t)\mathbf{Hc_{oi}^{\perp}},\ \forall i \in \mathcal{N}. \quad (25)$$

We find the dynamics of h_1 and h_2. The overall contribution of $\mathbf{u_i^s}$ is zero (Proposition 2), so we can write, for h_1:

$$\dot{h}_1 = \sum_{i \in \mathcal{N}} \frac{\partial h_1}{\partial \mathbf{q_i}}^T \mathbf{u_i^m} = \frac{k_c}{c_s} \sum_{i \in \mathcal{N}} \mathbf{c_{io}^T} z_i(t)\mathbf{Hc_{oi}^{\perp}} = -\frac{k_c}{c_s}z(t)h_2,$$

$$(26)$$

with $z(t) = -\sum_{i \in \mathcal{N}} z_i(t)\|\mathbf{c_{io}}\|^2$. Analogously, for h_2:

$$\dot{h}_2 = \sum_{i \in \mathcal{N}} \frac{\partial h_2}{\partial \mathbf{q_i}}^T \mathbf{u_i^m} = \frac{k_c}{c_s} \sum_{i \in \mathcal{N}} \mathbf{c_{io}^{\perp T}} z_i(t)\mathbf{Hc_{oi}^{\perp}} = \frac{k_c}{c_s}z(t)h_1.$$

$$(27)$$

The dynamics of s_h^2 (5) are $d(s_h^2)/dt = 2(h_1\dot{h}_1 + h_2\dot{h}_2)$. Substituting (26) and (27), one finds that $\dot{s}_h = 0$, i.e., the scaling parameter remains constant. ∎

These motions result, as one could expect, in behaviors for which the team and the grasped object gyrate. This can be interesting if the object needs to be rotated rigidly in the workspace due to task demands (i.e., for a subsequent treatment, or to place it in a prescribed absolute orientation).

B. Fixing the team's size and orientation using a single robot

A single *special robot* can steer the matrix $\mathbf{H}$ for the full team. Without loss of generality, let us assume that robot 1 is the special robot and $\mathbf{c_{1o}} \neq \mathbf{0}$. Consider the control:

$$\mathbf{u_1} = k_c \mathbf{d_1},\ \text{with}\ \mathbf{d_1} = \mathbf{q_{o1}} - \mathbf{H_1 c_{o1}}, \quad (28)$$

where $\mathbf{H_1}$ is a similarity. The following result holds:

Proposition 6: If all robots use the same control gain k_c, robots $i = 2, ..., N$ implement the standard control law (11), and robot $i = 1$ uses (28), then $\mathbf{H}$ tracks $\mathbf{H_1}$, according to: $\dot{\mathbf{H}} = -k_{f1}(\mathbf{H} - \mathbf{H_1})$, with $k_{f1} = k_c \cdot \|\mathbf{c_{1o}}\|^2/c_s$.

Proof: We look at the time derivative of $\mathbf{H}$. Let us define $\mathbf{H_{dif}} = \mathbf{H} - \mathbf{H_1}$ and $\mathbf{u_1} = \mathbf{u_1^s} + \mathbf{u_1^d}$, where $\mathbf{u_1^s}$ obeys (11) and $\mathbf{u_1^d} = k_c \mathbf{H_{dif} c_{o1}}$. From Prop. 2, the dynamics of $\mathbf{H}$ is due only to $\mathbf{u_1^d}$. Direct manipulations then lead to:

$$\dot{h}_1 = \frac{k_c}{c_s}\mathbf{c_{1o}^T} \mathbf{H_{dif} c_{o1}},\ \dot{h}_2 = \frac{k_c}{c_s}\mathbf{c_{1o}^{\perp T}} \mathbf{H_{dif} c_{o1}}. \quad (29)$$

Note that $\mathbf{H_{dif}}$ is a similarity. Using this constraint on its structure and developing the equations above, one can express the components of $\mathbf{H}$ back in matrix form and obtain:

$$\dot{\mathbf{H}} = -k_{f1}\mathbf{H_{dif}} = -k_{f1}(\mathbf{H} - \mathbf{H_1}). \quad (30)$$

∎

Thus, if $\mathbf{H_1}$ is constant, then $\mathbf{H}$ converges to it exponentially. If $\mathbf{H_1}$ is time-varying, then $\mathbf{H}$ tracks its variation. The special robot can in this way steer the value of $\mathbf{H}$. It can also control the team's geometric parameters (size and orientation) individually. Two possible strategies based on the controllers in Section V-A are described next.

S1: *Drive the team size s_h towards a desired value $s_h = s_1$, without changing $\mathbf{R_h}$:* Robots use (20), with $w_1(t) = s_1/s_h$ ($s_h > 0$ is assumed) and $w_i(t) = 1$ for $i = 2, ..., N$.

S2: *Rotate team towards a desired orientation $\mathbf{R_h} = \mathbf{R}(\alpha_1)$, without changing s_h:* Robots use (24), with $z_1(t) = k_{r1}(\alpha_1 - \alpha_h)$, $k_{r1} < 0$, and $z_i(t) = 0$ for $i = 2, ..., N$.

Notice that S1 and S2 are particular instances of the case studied in Prop. 6: robot 1 is enforcing a similarity $\mathbf{H_1}$,
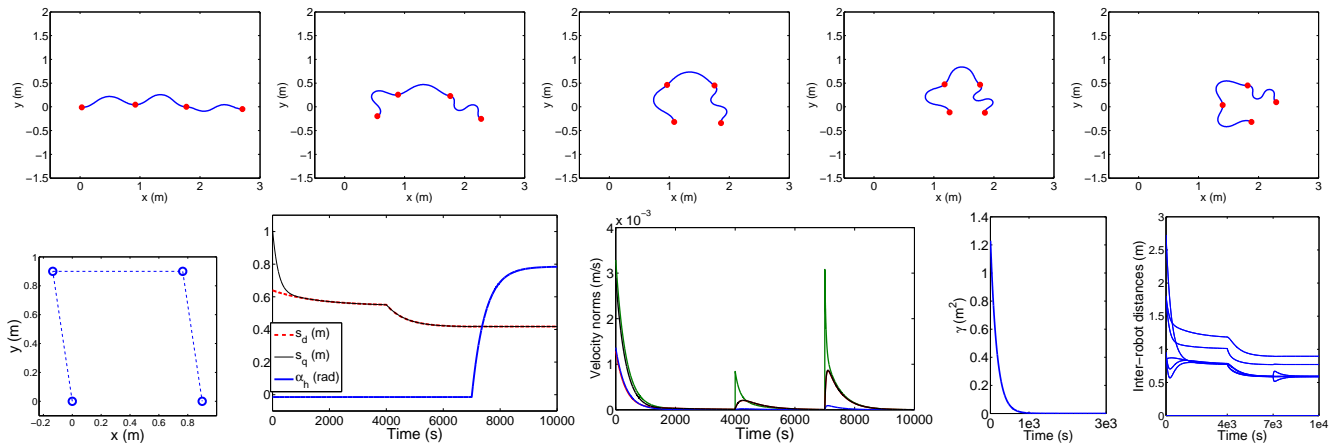
Fig. 2. Simulation results for linear object. Top: snapshots of object and robots (circles) evolution from initial (left) to final (right) configuration. Bottom, left to right: desired geometry (robots as circles); time evolution of: team sizes and similarity angle, robot speeds, cost function, and inter-robot distances.
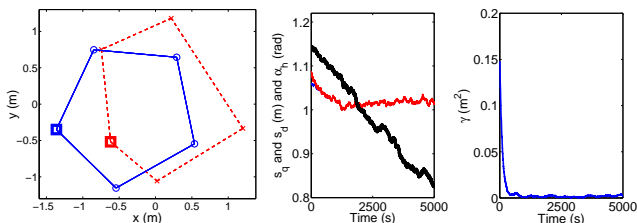

Fig. 3. Simulation example with five robots. Left to right: initial (robots joined by dashed lines) and final (solid lines) shapes, with one same robot marked with a square in both shapes; evolution of similarity angle (thickest line) and team sizes (thinner lines, with $s_q > s_d$); and of cost function.

which may be time-varying, while the other robots' motions minimize the deformation metric γ. As $\mathbf{H}$ will track $\mathbf{H_1}$, robot 1 can suitably steer the team's parameters.

The special robot may be a robot with superior perceptual/decision making capabilities, e.g., global positioning and environmental awareness to manipulate/transport the object avoiding obstacles; or a privileged agent whom we want to *lead* the task (e.g., as in human-robot collaboration). The other robots, meanwhile, can have more modest capabilities and rely on local reference frames and simpler sensors.

VI. SIMULATION STUDY

We present illustrative results of simulations, performed using MATLAB®. For our first example, we consider an inextensible elastic rod which rests in a planar workspace and is grasped rigidly at different points by four robots. Using gripping points along the rod –i.e., not just at its ends– makes it easier to steer this type of object around environmental obstacles and to control its shape precisely. We employ a quasi-static model of the rod's state based on minimal-energy configurations, as in previous works, e.g., [16], [17].

We control the orientation of the grippers/robots with a simple strategy aimed at avoiding sharp curvatures of the rod. We use for $\theta_i \in (-\pi, \pi]$ –the orientation of robot i, equal to the tangent angle of the rod at that robot's position–:

$$\dot{\theta}_i = k_{ai}(\theta_i^d - \theta_i), \qquad (31)$$

with $k_{ai} > 0$ a control gain, $\theta_i^d = \angle(\overline{\mathbf{q_{i,i-1}}} + \overline{\mathbf{q_{i+1,i}}})$ for $i = 2, ..., N-1$, $\theta_1^d = \angle(\overline{\mathbf{q_{21}}})$, $\theta_N^d = \angle(\overline{\mathbf{q_{N,N-1}}})$. Here, $\angle(\cdot)$ denotes the angular polar coordinate of a vector and $\overline{\cdot}$ the normalization to unit. Figure 2 illustrates the test's results.

Initially, the rod was fairly stretched out. The prescribed shape we chose was close to that of a square. The controllers used were those described in Section V-B. Robot 1 (leftmost at the start of execution) acted as the special robot. Three control phases were executed. First, robot 1 specified a team size (strategy S1). Then, it commanded a reduction of size with no rotation (S1). Finally, it made the team rotate without changing size (S2). The team parameters evolved as theoretically expected. The robot motions were efficient and the changes in the object's shape were smooth.

Our second simulation example, aimed at testing the robustness of the controller, included additive Gaussian noise both in the measurement and the actuation for all robots, and a systematic error added to the velocity of one robot. Five robots with a regular pentagonal desired shape were used. No object was considered in the simulation. Robots followed S1 so as to fix a desired team size $s_1 = s_d = 1$. As is observable in Fig. 3, the controller was able to keep the team close to the desired shape despite the perturbations. The deformation metric γ was maintained in low values. A complementary video provides further illustration of the simulation results.

VII. CONCLUSION

We believe that the main appeal of the proposed method is that it applies multirobot formalisms to the control of metrics of deformation. This links it with object manipulation tasks and opens the door to multiple potentially interesting applications. However, several essential issues were not considered. We do not address the interaction with the object; for precise and safe operation, information of force and object state should be included in the control loop. Also, if the desired shape is very different from the initial one, it would be necessary to use additional planning. Finally, robot dynamics constraints, control in 3D space, and collision avoidance guarantees can be studied building on the presented results.

REFERENCES

[1] D. Sieber, F. Deroo, and S. Hirche, "Iterative optimal feedback control design under relaxed rigidity constraints for multi-robot cooperative manipulation," in *IEEE Conference on Decision and Control*, 2013, pp. 971–976.

[2] D. Berenson, "Manipulation of deformable objects without modeling and simulating deformation," in *IEEE/RSJ International Conference on Intelligent Robots and Systems*, 2013, pp. 4525–4532.

[3] J. Umlauft, D. Sieber, and S. Hirche, "Dynamic movement primitives for cooperative manipulation and synchronized motions," in *IEEE International Conf. on Robotics and Automation*, 2014, pp. 766–771.

[4] J. C. Gower and G. B. Dijksterhuis, *Procrustes problems*. Oxford University Press, 2004.

[5] H. Bai and J. T. Wen, "Cooperative load transport: A formation-control perspective," *IEEE Transactions on Robotics*, vol. 26, no. 4, pp. 742–750, 2010.

[6] F. Basile, F. Caccavale, P. Chiacchio, J. Coppola, and C. Curatella, "Task-oriented motion planning for multi-arm robotic systems," *Robotics and Computer-Integrated Manufacturing*, vol. 28, no. 5, pp. 569–582, 2012.

[7] J. Markdahl, Y. Karayiannidis, X. Hu, and D. Kragic, "Distributed cooperative object attitude manipulation," in *IEEE International Conference on Robotics and Automation*, 2012, pp. 2960–2965.

[8] Z. Wang and M. Schwager, "Kinematic multi-robot manipulation with no communication using force feedback," in *IEEE International Conference on Robotics and Automation*, 2016, pp. 427–432.

[9] A. Petitti, A. Franchi, D. D. Paola, and A. Rizzo, "Decentralized motion control for cooperative manipulation with a team of networked mobile manipulators," in *IEEE International Conference on Robotics and Automation*, 2016, pp. 441–446.

[10] H. G. Tanner, S. G. Loizou, and K. J. Kyriakopoulos, "Nonholonomic navigation and control of cooperating mobile manipulators," *IEEE Trans. on Robotics and Automation*, vol. 19, no. 1, pp. 53–64, 2003.

[11] J. Alonso-Mora, R. Knepper, R. Siegwart, and D. Rus, "Local motion planning for collaborative multi-robot manipulation of deformable objects," in *IEEE International Conference on Robotics and Automation*, 2015, pp. 5495–5502.

[12] K.-K. Oh, M.-C. Park, and H.-S. Ahn, "A survey of multi-agent formation control," *Automatica*, vol. 53, pp. 424–440, 2015.

[13] J. Sanchez, J.-A. Corrales, B.-C. Bouzgarrou, and Y. Mezouar, "Robotic manipulation and sensing of deformable objects in domestic and industrial applications: a survey," *The International Journal of Robotics Research*, vol. 37, no. 7, pp. 688–716, 2018.

[14] J. Das and N. Sarkar, "Autonomous shape control of a deformable object by multiple manipulators," *Journal of Intelligent & Robotic Systems*, vol. 62, no. 1, pp. 3–27, 2011.

[15] P. Jiménez, "Survey on model-based manipulation planning of deformable objects," *Robotics and Computer-Integrated Manufacturing*, vol. 28, no. 2, pp. 154–163, 2012.

[16] T. Bretl and Z. McCarthy, "Quasi-static manipulation of a Kirchhoff elastic rod based on a geometric analysis of equilibrium configurations," *The International Journal of Robotics Research*, vol. 33, no. 1, pp. 48–68, 2014.

[17] M. Mukadam, A. Borum, and T. Bretl, "Quasi-static manipulation of a planar elastic rod using multiple robotic grippers," in *IEEE/RSJ Int. Conf. on Intelligent Robots and Systems*, 2014, pp. 55–60.

[18] A. Delgado, J.-A. Corrales, Y. Mezouar, L. Lequievre, C. Jara, and F. Torres, "Tactile control based on Gaussian images and its application in bi-manual manipulation of deformable objects," *Robotics and Autonomous Systems*, vol. 94, pp. 148–161, 2017.

[19] D. Navarro-Alarcón, Y. Liu, J. G. Romero, and P. Li, "Model-free visually servoed deformation control of elastic objects by robot manipulators," *IEEE Transactions on Robotics*, vol. 29, no. 6, pp. 1457–1468, 2013.

[20] D. Navarro-Alarcón and Y. Liu, "Fourier-based shape servoing: A new feedback method to actively deform soft objects into desired 2-D image contours," *IEEE Transactions on Robotics*, vol. 34, no. 1, pp. 272–279, 2018.

[21] Z. Hu, P. Sun, and J. Pan, "Three-dimensional deformable object manipulation using fast online Gaussian process regression," *IEEE Robotics and Automation Letters*, vol. 3, no. 2, pp. 979–986, 2018.

[22] K. Kanatani, "Analysis of 3-D rotation fitting," *IEEE Trans. Pattern Anal. Mach. Intell.*, vol. 16, no. 5, pp. 543–549, 1994.

[23] M. Aranda, G. López-Nicolás, C. Sagüés, and M. M. Zavlanos, "Coordinate-free formation stabilization based on relative position measurements," *Automatica*, vol. 57, pp. 11–20, 2015.

[24] C. Ze-Su, Z. Jie, and C. Jian, "Formation control and obstacle avoidance for multiple robots subject to wheel-slip," *Int. Journ. Advanced Robotic Syst.*, vol. 9, no. 5, pp. 188–202, 2012.

[25] A. R. Mosteo, E. Montijano, and D. Tardioli, "Optimal role and position assignment in multi-robot freely reachable formations," *Automatica*, vol. 81, pp. 305–313, 2017.